Engineering e-Transaction (ISSN 1823-6379)
Vol. 7, No.2, December 2012, pp 96-106
Online at http://ejum.fsktm.um.edu.my
Received 16 Oct, 2012; Accepted 20 Dec, 2012

MULTIPLE STABLE SOLUTIONS FOR TWO-AND FOUR-SIDED LID-DRIVEN CAVITY FLOWS USING FAS MULTIGRID METHOD

D.S. Kumar[a], A.K. Dass[a] and A. Dewan[b]
[a]Department of Mechanical Engineering, Indian Institute of Technology Guwahati,
Guwahati - 781039, India
[b]Department of Applied Mechanics, Indian Institute of Technology Delhi
New Delhi - 110016, India
Email: d.kumar@iitg.ac.in

ABSTRACT

The present work is concerned with the computations of two- and four-sided lid-driven square cavity flows to obtain multiple steady solutions using a time-efficient FAS multigrid code based on the SIMPLE algorithm on a colocated grid arrangement. The transport equations are discretized using the QUICK scheme for the convective terms and central-difference scheme for the viscous and the pressure gradient terms. The code is first validated against existing results for a single-sided lid-driven square cavity flow. It is then applied to the two- and four-sided lid-driven cavity flows that involve multiple stable solutions. In the two-sided square cavity two of the adjacent walls move with an equal velocity and in the four-sided cavity all the four walls move in such a way that parallel walls move in the opposite directions with the same velocity. The resulting flow fields show that a symmetric solution exists for all Reynolds numbers whereas multiplicity of states of one symmetric and two asymmetric solutions for the two- and four-sided cavity flows are identified above the critical Reynolds number. The strategy employed to obtain these solutions is described. For the first time a multigrid strategy is employed to capture multiple steady states.

Keywords: Incompressible flows; lid-driven cavity; finite-volume method; multiple solution; multigrid method.

1.0 INTRODUCTION

In the past two decades the Semi Implicit Method for Pressure Linked Equation (SIMPLE) algorithm is probably the most widely used method for the calculation of incompressible flows. The SIMPLE algorithm of Patankar and Spalding (1972) is used to couple the momentum and continuity equations. In this method, the discretized equations for velocity components and a pressure correction equation are solved in a sequential manner. The pressure correction formulation which is used to link the pressure and the velocity fields, however, is weak and leads to slow convergence or even divergence if appropriate under-relaxations are not used. A major factor affecting the performance of a scheme is its ability to smoothen out the errors of all frequencies effectively in the solution. Iterative methods, such as line-by-line solvers, provide excellent smoothening of the errors of wavelengths comparable to the mesh size. As the grid is refined, these solvers show fast convergence in the initial few iterations, but subsequently the convergence rate deteriorates rapidly. This is due to the persistence of low-frequency errors that are not effectively smoothened by the repeated relaxation sweeps on a given grid.

The multigrid methods exploit the ability of relaxation procedures to efficiently smoothen the errors of wavelengths comparable to the mesh size, by employing a hierarchy of grids. By solving the equations at different grid levels, the errors of all frequencies are smoothened. The multilevel principle can be used to accelerate the convergence of the sequential as well as the coupled procedures. However, the ability of the coupled procedures to implicitly retain the velocity-pressure coupling makes the multilevel application to the coupled solvers quite attractive. Fedorenko (1962, 1964) is the originator of the idea of multigrid which initially did not draw much attention. Interest in the technique was reawakened later by Brandt (1977). He also gave it a sound mathematical foundation in a path-breaking paper in 1977. He was the first to demonstrate the practical efficiency and generality of the multigrid methods. The multigrid method was discovered independently by Hackbusch (1978) at about the same time, who laid firm mathematical foundations and provided reliable

methods. Multigrid methods have been analysed, applied and generalized in many ways since their introduction, and are gradually becoming recognized as a powerful tool in applied mathematics. Sivaloganathan and Shaw (1988) applied multigrid method to SIMPLE pressure correction technique of Patankar and Spalding using staggered grid. They adopted the full-approximation storage multigrid method and achieved a large reduction in CPU time. Since then application of multigrid method in SIMPLE pressure correction smoothers has increased.

Grid-coarsening process is difficult in staggered grid arrangement because of the use of three different set of cells. Hence a colocated grid layout is used in the present work. The momentum interpolation proposed by Rhie and Chow (1983) is employed in the present work for calculating the cell-face mass fluxes to avoid pressure oscillations. Hortman and Peric (1990) presented a finite volume multigrid procedure for the prediction of laminar natural convection flows, enabling efficient and accurate calculations on very fine grids. Lien and Leschziner (1994) investigated the effectiveness of a number of multigrid convergence acceleration algorithms, implemented within a colocated finite volume solver for laminar and turbulent flows. A dramatic reduction in the computational time using the multigrid method was showed by Hortmann and Peric (1990); Lien and Leschziner (1994). Yan and Thiele (1998) developed a modified full multigrid algorithm in which only residuals are restricted from the fine to coarse grid by summation but not the variables. This simplifies the multigrid strategy and the structure of the program. Yan and Thiele (1998) solved fluid flows with heat transfer using SIMPLE algorithm on colocated grids.

Recently, Santhosh et al. (2009) applied FAS multigrid method in porous cavity flows and showed a significant acceleration in convergence over single-grid methods. The FAS multigrid code developed in the present work for one-sided lid-driven cavity exhibits fast convergence and accuracy. The present results are compared with well-established results. After having thus gained confidence in the code it is then applied to compute the multiple solutions for two-sided and four-sided lid-driven cavities.

Kuhlmann et al. (1997, 1998) extended the one-sided lid driven cavity problem to a two-sided problem, where the flow is driven by the parallel or anti-parallel motion of two facing walls. The facing walls could be either the left and right walls or the upper and lower walls. At low Reynolds number, the flow consists of separate co- or counter-rotating primary vortices that form adjacent to each moving wall. At higher Reynolds numbers, instabilities arise in the flow due to the interaction between the two primary vortices. Moreover, their results showed that multiple flow solutions may exist, depending on the cavity aspect ratio and the value of the Reynolds number (Albensoeder et al. 2001). Recently, Cadou et al (2012) and Namprai et al (2102) have done stability analysis for the square cavity problems.

Numerical simulations of two-sided lid driven cavity flow with temperature gradient and accompanied by heat and mass transport were also reported by Alleborn et al. (1999) and Luo and Yang (2007). More recently, the multiplicity of flow states induced by the motion of two-sided non-facing lid-driven cavity flow and four-sided lid-driven cavity flow have been investigated by Wahba (2009). He found the critical Reynolds number of 1073 for the two-sided lid-driven cavity and 129 for the four-sided lid-driven cavity. We have reproduced the results of Wahba (2009) in addition to the pressure contours to show the ability and accuracy of multigrid method that the symmetric solution exists for all Reynolds numbers, whereas multiplicity of states of one symmetric and two asymmetric solutions for the two-sided and four-sided cavity flows are identified above the critical Reynolds number. Here we have captured multiple steady solutions at post-critical Reynolds numbers for both the two-sided and four-sided cavity flows using FAS multigrid method. The strategy employed to obtain these solutions is also described. The paper is organized in four sections. Section 2 describes the non-dimensional governing equations and numerical method. Section 3 deals with results and discussion and in Section 4 we list our observations and conclusions.

2.0 GOVERNING EQUATIONS AND NUMERICAL METHOD

The flow is considered to be laminar and incompressible. The fluid physical properties are assumed to be constant. Under these assumptions, the

governing equations in the traditional primitive variable formulation in the non-dimensional form can be written as

$$\frac{\partial u}{\partial x}+\frac{\partial v}{\partial y}=0 \qquad (1)$$

$$u\frac{\partial u}{\partial x}+v\frac{\partial u}{\partial y}=-\frac{\partial p}{\partial x}+\frac{1}{\mathrm{Re}}\left[\frac{\partial^2 u}{\partial x^2}+\frac{\partial^2 u}{\partial y^2}\right] \qquad (2)$$

$$u\frac{\partial v}{\partial x}+v\frac{\partial v}{\partial y}=-\frac{\partial p}{\partial y} \qquad (3)$$

Here u and v denote the velocities along x- and y-directions and p the pressure, respectively. The dimensionless governing equations for a general field variable ϕ for steady flow can be written as

$$\frac{\partial}{\partial x}(u\phi)+\frac{\partial}{\partial y}(v\phi)=\frac{\partial}{\partial x}\left(\Gamma^{\phi}\frac{\partial \phi}{\partial x}\right)+\frac{\partial}{\partial y}\left(\Gamma^{\phi}\frac{\partial \phi}{\partial y}\right)+S^{\phi} \qquad (4)$$

Where ϕ is the dependent variable and, Γ^{ϕ} and S are the diffusion coefficient and source term, respectively. The following substitutions in Equation (4) give the continuity equation:

$$\phi=1,\ \Gamma^{\phi}=0,\ S^{\phi}=0 \qquad (5)$$

The x-momentum equation results from the substitution

$$\phi=u,\ \Gamma^{\phi}=\frac{1}{\mathrm{Re}},\ S^{\phi}=-\frac{\partial p}{\partial x} \qquad (6)$$

and the y-momentum equation results from the substitution

$$\phi=v,\ \Gamma^{\phi}=\frac{1}{\mathrm{Re}},\ S^{\phi}=-\frac{\partial p}{\partial y} \qquad (7)$$

The governing equations are discretized using the finite volume method (FVM) on a colocated grid arrangement. An attractive feature of this method is that the solution would satisfy the integral conservation of mass, momentum and other quantities over any group of control volumes and of course over the whole computational domain. Since the momentum equations are integrated over the colocated control volumes, Rhie and Chow (1983) interpolation is used to ensure strong pressure-velocity coupling. To improve the guessed pressure, pressure-correction equation derived from the continuity equation is used. In order to overcome the instability that arises due to the central-difference scheme, higher-order Quadratic Upwind Interpolation for Convective Kinematics (QUICK) scheme is used to discretize the convective part of the governing equations and central-differences are used to compute the diffusive fluxes and the pressure gradient.

2.1 Discretization Method

In the cell-centred finite volume method used here the calculation domain is divided into a number of non-overlapping control volumes such that all flow variables 'sit' at the centre of the control volume. The differential equation integrated over each control volume yields a discretized equation at each cell-centre. The convective fluxes at the cell interfaces are computed using the QUICK scheme and the diffusive fluxes by central differences. The Quadratic Upwind Interpolation for Convective Kinematics (QUICK) scheme was devised by Leonard (1979). It uses the quadratic interpolation between two upstream neighbours and one downstream neighbour to evaluate ϕ (and hence flux) at the control volume interfaces. The value of ϕ at the east face e of the control volume is given by the quadratic interpolation.

$$\phi_e=\frac{3}{8}\phi_E+\frac{3}{4}\phi_P-\frac{1}{8}\phi_W \quad if\ \ F_e>0 \qquad (8)$$

$$\phi_e=\frac{3}{8}\phi_P+\frac{3}{4}\phi_E-\frac{1}{8}\phi_{EE} \quad if\ \ F_e<0 \qquad (9)$$

Where $F_e = u\Delta y$ represents the convection strength, which is positive for convection in the positive x-direction. Therefore the convective flux term can be expressed as

$$F_e\phi_e=\left(\frac{3}{8}\phi_E+\frac{3}{4}\phi_P-\frac{1}{8}\phi_W\right)\left[\left|0,F_e\right|\right]-\left(\frac{3}{8}\phi_P+\frac{3}{4}\phi_E-\frac{1}{8}\phi_{EE}\right)\left[\left|0,-F_e\right|\right] \qquad (10)$$

Where the operator $[|x, y|]$ denotes the maximum of the two arguments x and y. The deferred QUICK scheme (Hayase et al. 1992) employed in the present work is given by

$$F_e\phi_e=\left(\phi_P^n+\frac{1}{8}\left(3\phi_E-2\phi_P-\phi_W\right)^{n-1}\right)\left[\left|0,F_e\right|\right]-\left(\phi_E^n+\frac{1}{8}\left(3\phi_P-2\phi_E-\phi_{EE}\right)^{n-1}\right)\left[\left|0,-F_e\right|\right] \qquad (11)$$

Where the superscript n represents the latest value of the variable and $n-1$ represents the value of the variable in the previous iteration. The description of

multigrid algorithm is explained by the same author in Santhosh et al. (2009).

3.0 RESULTS AND DISCUSSION

3.1 Application to Lid-Driven Cavity Flow

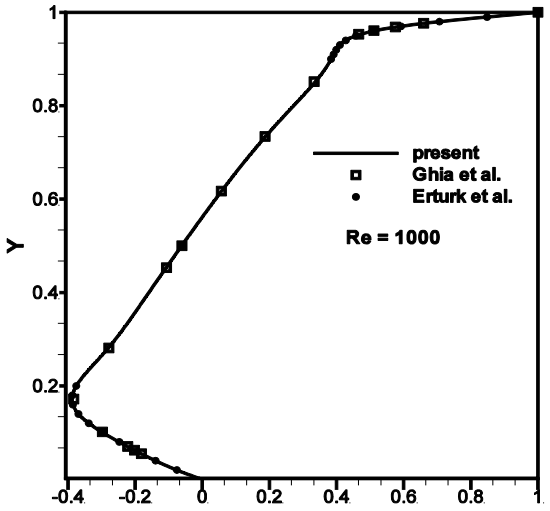
A computer code has been developed using the QUICK scheme for convective terms and central-difference scheme for the viscous terms. In order to evaluate the performance of the code, it has been applied to a standard test problem, namely, 2D single-sided lid-driven cavity, where the fluid in a square cavity is set into motion by the movement of one wall. This problem is the most frequently used benchmark for the assessment of numerical methods particularly for the steady state solution of the incompressible viscous flows (Ghia et al., 1982.; Bruneau and Jouron, 1990; Barragy and Carey, 1997; Botella and Peyret, 1998; Kalita et al., 2002; Auteri et al., 2002; Bruneau and Saad, 2006). Since steady equations are solved using the SIMPLE algorithm in the present work, the developed code captures only the final steady-state results. The dimensionless boundary conditions are given as

$$x = 0 : u = 0.0, v = 0.0$$
$$x = 1 : u = 0.0, v = 0.0$$
$$y = 0 : u = 0.0, v = 0.0$$
$$y = 1 : u = 1.0, v = 0.0$$

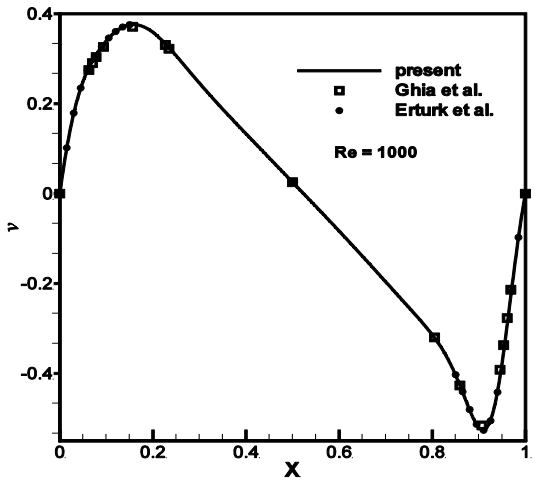
The moving wall generates vorticity which diffuses inside the cavity and this diffusion is the driving mechanism of the flow. At high Reynolds numbers, several secondary and tertiary vortices begin to appear, whose characteristics depend on Re.

Figure 1 presents a comparison of the steady-state horizontal velocities on the vertical centreline and the vertical velocities on the horizontal centreline of the square cavity with those obtained by Ghia et al. (1982) and Erturk et al. (2005) and the agreement is quite good. It is seen that the results produced by the present FAS multigrid code are accurate and the code stands validated.

Now we carry out a comparison exercise to evaluate the performance of the 4- level multigrid versus the single-grid method. Expectedly full-approximation storage multigrid method shows a faster convergence. All the results presented here are produced using a 4-level V-cycle strategy and increasing the level further does not pay any additional dividend. The computational effort is reported in terms of equivalent fine-grid sweeps that are



(a)



(b)

Fig. 1 Comparison of steady-state velocity profiles (a) Horizontal velocity along the vertical centreline and (b) Vertical velocity along the horizontal centerline for the single-sided lid-driven cavity.

usually referred to as work units. Figure 2 gives the comparison between 4-level multigrid and single-grid for the history of mass residual on a 130 × 130 grids. Expectedly a 4-level multigrid cycle shows a faster convergence than a single grid. Figure 2 shows that in the single-grid the residuals fall faster at the beginning and slows down thereafter whereas in multigrid method the residual falls at a more or less constant rate. It is observed that work units required to reach the

steady state increase as *Re* increases for both single grid and multigrid. This can be attributed to the fact that high Reynolds number flows contain multiplicity of scales, which introduce high frequency errors into the computational process.

Table 1 summarizes the total CPU time required and speedup obtained by multigrid for various Reynolds numbers. For the same fall of residual, time-gain by multigrid is impressive. The time-wise speed-up achieved by multigrid at 'steady state' is approximately 8 to 10 times for the various Reynolds numbers. All the CPU times given in Table 1 correspond to the computations carried out on a Dual Xeon 3.2 GHz based machine. Thus, in terms of computational efficiency, the 4-level multigrid method is substantially faster than the single grid method.

Table 1 Performance of multigrid method for a single-sided lid-driven cavity flow at various Reynolds numbers.

Reynolds number	CPU time (minutes)		Speed-up
	Single-grid	MG 4-level	
1000	262	25	10.41
3200	644	81	7.95
5000	1048	130	8.06
7500	1425	158	9.01

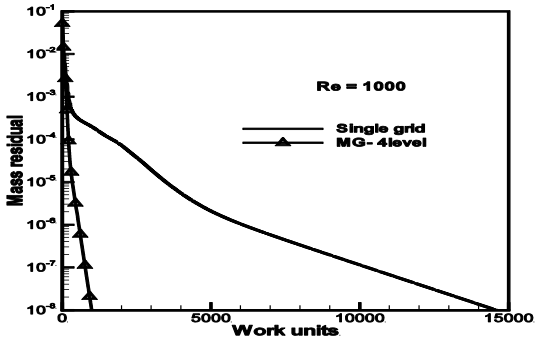
3.2 Multiple Solutions for Two- and Four-Sided Lid-Driven Cavity Flows

3.2.1 Two-Sided Non-Facing Lid-Driven Cavity Flow

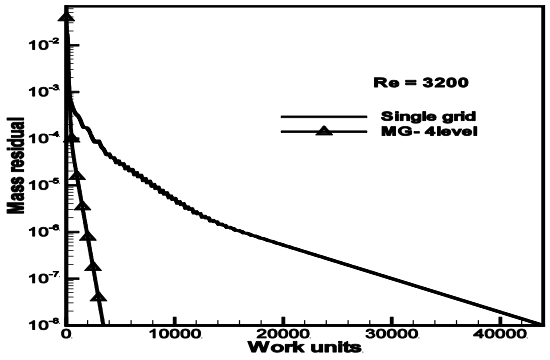
The flow configuration for the two-sided non-facing lid-driven cavity is shown in Figure 3. The dimensionless boundary conditions are given as

$$x = 0 : u = 0.0, v = -1.0$$
$$x = 1 : u = 0.0, v = 0.0$$
$$y = 0 : u = 0.0, v = 0.0$$
$$y = 1 : u = 1.0, v = 0.0$$

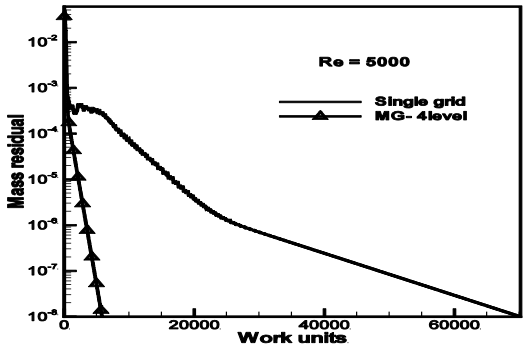
Here the flow is driven by the upper wall (y = 1) moving from the left to right and the left wall moving downwards. The top wall drags the fluid to the right and this fluid then gets deflected by the right wall that makes the fluid rotate in the clockwise direction. Similarly the left wall drags the fluid to the bottom and it is deflected by the bottom wall that makes the fluid rotate in the counterclockwise direction. Apart from the two counter-rotating primary vortices, two secondary vortices are formed with the resulting flow field being symmetric about the diagonal passing through the point



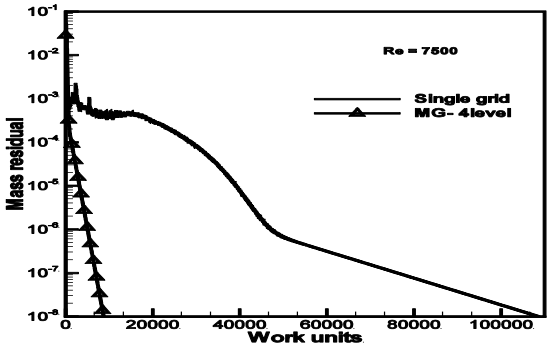
(a)



(b)



(c)



(d)

Fig. 2 Mass residual history of multigrid methods for single-sided lid-driven cavity for various Reynolds numbers.

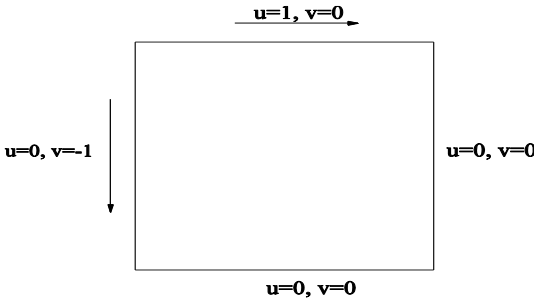
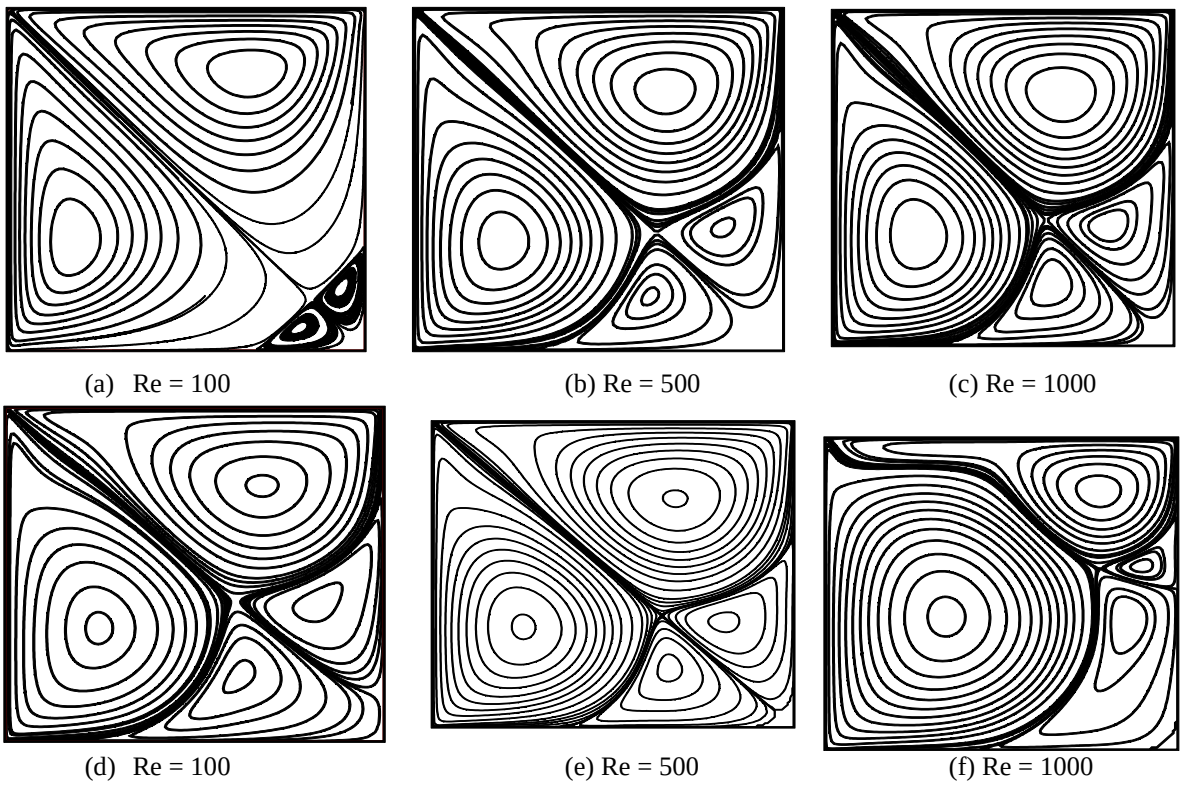


Fig. 3 Schematic diagram of the two-sided lid-driven cavity.

where the moving walls meet. As *Re* increases to a critical value and beyond, the flow produces multiple symmetric and asymmetric steady solutions that depend upon the sweeping direction in the line-by-line iterative solver.

Figure 4 shows a few streamline patterns for various Reynolds numbers. At lower Reynolds numbers [Figure 4(a-c)] the streamline patterns are symmetric about a diagonal and as the Reynolds number increases, the size of the secondary vortices grow in size at the expense of the primary vortices. As seen from Figure 4 (d-f) at larger Reynolds numbers asymmetry may develop. Recently Wahba (2009) showed that between Reynolds number values of 1071 and 1075, the flow bifurcates from a stable symmetric state to a stable asymmetric state and the critical Reynolds number for flow bifurcation in two-sided non-facing lid-driven cavity is 1073. Figure 4(d) shows that at Re = 1075 there is a departure from the symmetry with the upper vortices becoming lightly smaller than the corresponding lower ones if the sweeping direction in the line-by-line iterative solver is from the left to right and our result is consistent with those reported by Wahba (2009). This trend continues with an increase in *Re* with the result that at *Re* = 1500 and 2000 [Figure 4 (e-f)] the upper vortices are considerably larger than the corresponding lower ones. If the sweeping direction is reversed the resulting asymmetric flow patterns have upper vortices larger than the corresponding lower ones.

Figure 5 shows the multiple-steady flow patterns with one symmetric and two asymmetric solutions at *Re* = 2000. The first asymmetric solution [Figure 5(a)] is obtained when the line-by-line solver sweeps from the left to right. If the direction of sweep is reversed another asymmetric solution [Figure 5(b)] is obtained.

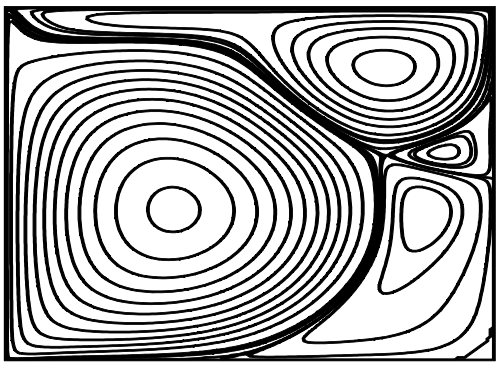


(a) Re = 100 (b) Re = 500 (c) Re = 1000

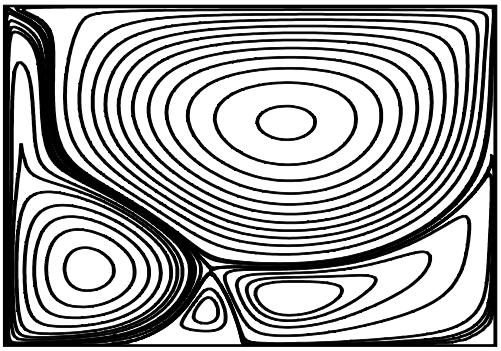
(d) Re = 100 (e) Re = 500 (f) Re = 1000

Fig. 4 Steady state streamline patterns for the two-sided lid-driven cavity for different Reynolds numbers.

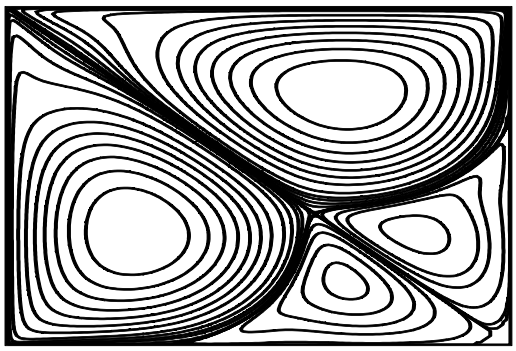
That both these asymmetric patterns are valid stable solutions to the problem can be gauged from the fact that there is no change of state if the final solution obtained by sweeping in one direction is given as the input to the solver sweeping in the other direction.



(a) Asymmetric (1)



(b) Asymmetric (2)



(c) Symmetric

Fig. 5 Multiple solutions for a two-sided lid-driven cavity at *Re* = 2000.

The flow geometry clearly suggests the existence of a symmetric solution as well. Figure 5(c) shows this flow pattern, which is obtained by putting u = - v on the symmetry diagonal from the beginning to the point when the mass residual reaches a value of 10^{-3} so as to help the flow develop in the direction that favours the desired solution. After this artificial restriction is removed to obtain a valid solution, the mass residual is allowed to fall below 10^{-8} when Figure 5(c) is plotted.

3.2.2 Four-Sided Lid-Driven Cavity Flow

A schematic representation of the four-sided lid-driven cavity is shown in Figure 6. The dimensionless boundary conditions are given by

$$x = 0 : u = 0.0, v = -1.0$$
$$x = 1 : u = 0.0, v = 1.0$$
$$y = 0 : u = -1.0, v = 0.0$$
$$y = 1 : u = 1.0, v = 0.0$$

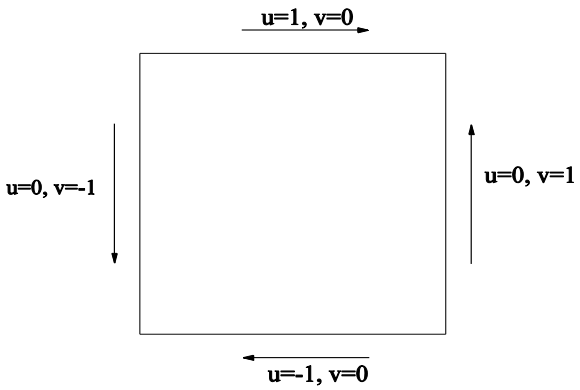


Fig. 6 Schematic diagram of the four-sided lid-driven cavity.

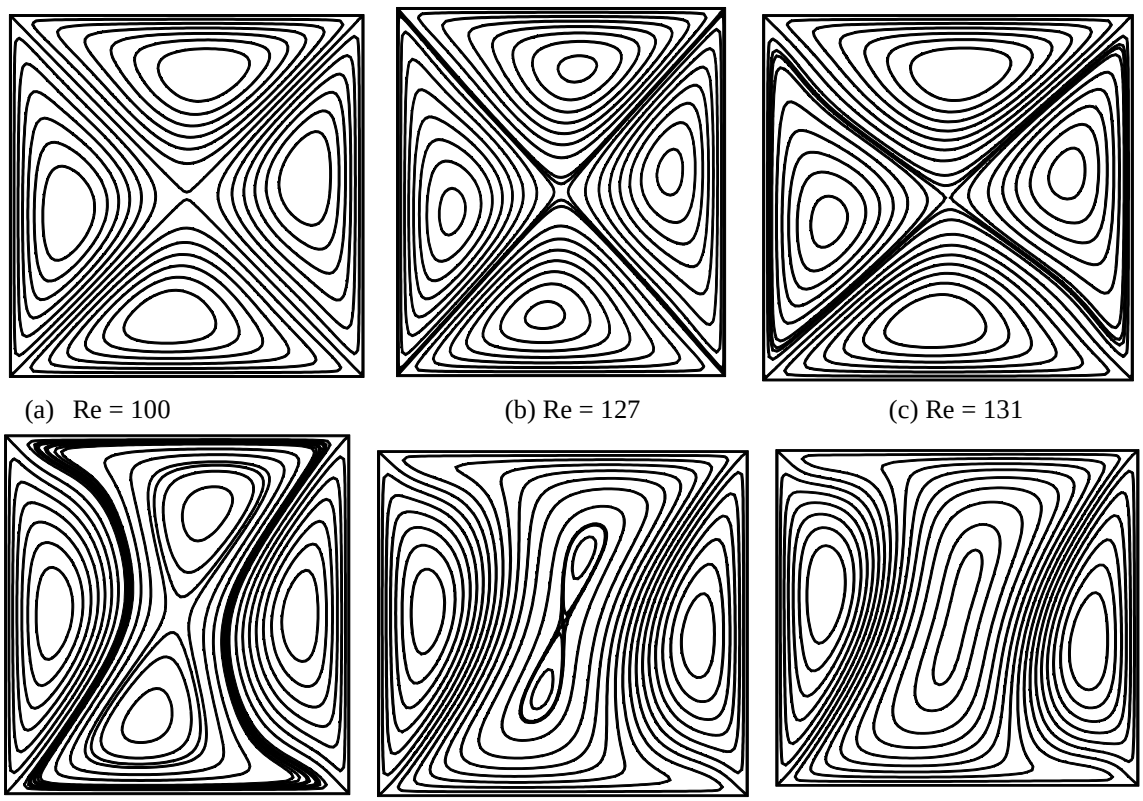
Here the upper and the lower walls move to the right and left respectively, while the left wall moves downwards and the right wall upwards. All the four walls move with equal speeds. The top wall drags the fluid to the right and this fluid is then deflected by the right wall that makes the fluid rotate in the clockwise direction. The right wall drags the fluid upwards and the fluid is then deflected by the top wall so that it rotates in the counterclockwise direction. Similarly, the bottom wall moving to the left and the left wall moving downwards make the dragged fluid rotate in the clockwise and counterclockwise directions, respectively. Since all the four walls move with equal speed, four distinct vortices of similar size develop symmetric to both the diagonals.

Figure 7 shows a few streamline patterns for various Reynolds numbers. At *Re* = 100 and *Re* = 127 [Figure 7(a-b)] the streamline patterns are symmetric about both the diagonals. As seen from Figure 7 (c-f) at larger Reynolds number asymmetry may develop. For a four-sided lid-driven cavity Wahba (2009) showed that between Reynolds number values of 127 and 131,

the flow bifurcates from a stable symmetric state to a stable asymmetric state and the critical Reynolds number for bifurcation in four-sided lid-driven cavity is 129. Figure 7 (c) shows that at *Re* = 131 there is a departure from the symmetry with the upper and lower vortices showing a tendency to merge into one if the line-by-line iterative solver sweeps vertically and our result is consistent with those reported in Wahba (2009). The merging process continues with the increase in *Re* as can be seen from Figure 7 (d-f). Figure 7 (f) shows a state when the merging results in a single vortex with a single core. This vortex is considerably larger than the right and left vortices. If a horizontal line-by-line sweep is employed instead of a vertical sweep the resulting asymmetric flow patterns would have merged right and left vortices and the resultant vortex would be larger than the upper and lower vortices.

Figure 8 shows the multiple-steady flow patterns with one symmetric and two asymmetric solutions at *Re* = 200. The first asymmetric solution (Figure 8(a)) is obtained when the line-by-line solver sweeps from the left to right. If the direction of sweep is changed to vertical another asymmetric solution Figure 8(b) is obtained. That both these asymmetric patterns are valid stable solutions to the problem can be gauged from the fact that there is no change of state if the final solution obtained by sweeping in one direction is given as the input to the solver sweeping in the other direction. The flow geometry clearly suggests the existence of a symmetric solution as well. Figure 8 (c) shows this flow

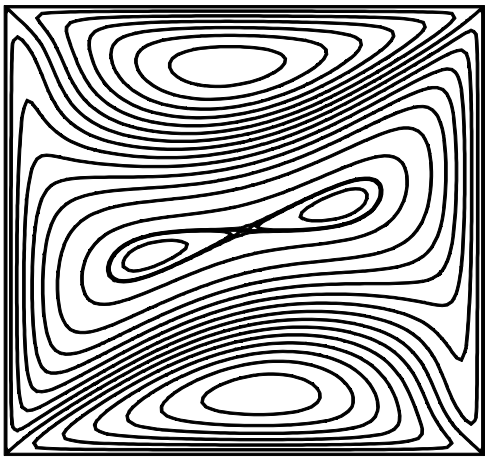
pattern, which is obtained by putting u = − v on the symmetry diagonal from the top-left to the bottom-right corner and putting u = v on the symmetry diagonal from the bottom-left to the top-right corner till when the mass residual reaches a value of 10^{-3} so as to help the flow develop in the direction that favours the desired solution. After this artificial restriction is removed to obtain a valid solution, the mass residual is allowed to fall below 10^{-8} when Figure 8(c) is plotted.



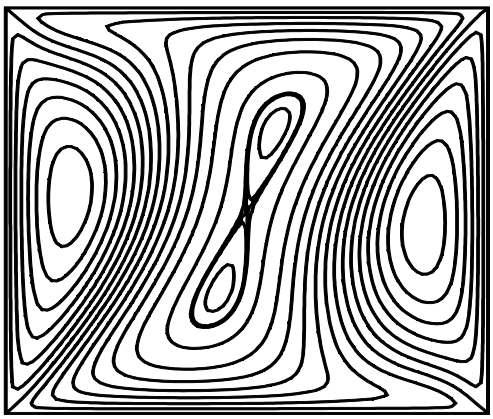
(a) Re = 100 (b) Re = 127 (c) Re = 131

(e) Re = 150 (e) Re = 200 (f) Re = 300

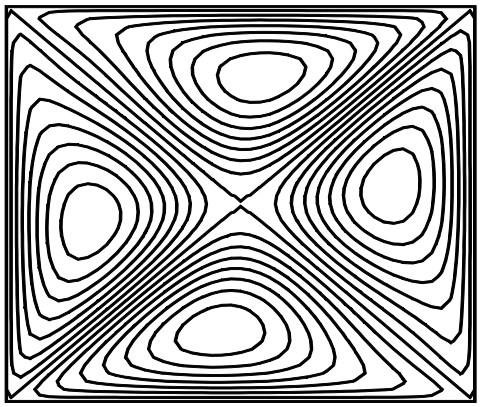
Fig. 7 Steady state streamline patterns for the four-sided lid-driven cavity for different Re.



(a) Asymmetric(1)



(b) Asymmetric(2)

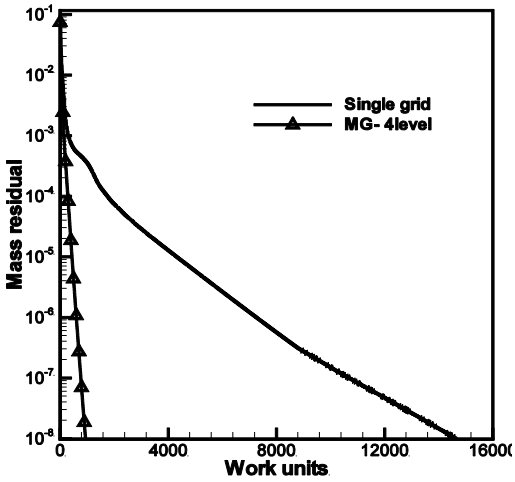


(c) symmetric

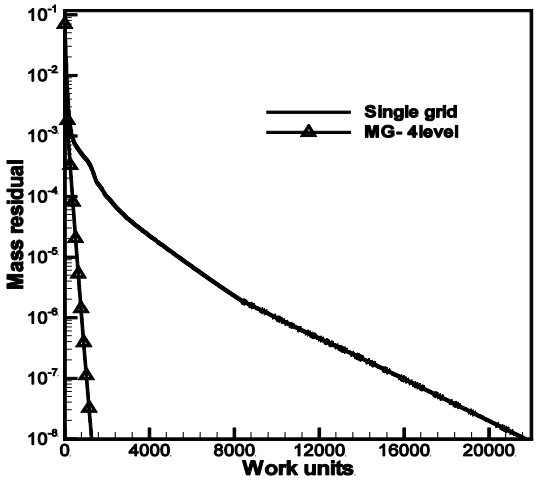
Fig. 8 Multiple solutions for a four-sided lid-driven cavity at *Re* = 200.

3.3 Multigrid Performance

Now we carry out a comparison exercise to evaluate the performance of the 4-level multigrid versus the single-grid method for two-sided and four-sided lid-driven cavities. Figure 9 provides for the two-sided lid-driven cavity the comparison between 4-level multigrid and single-grid for the history of mass residual on a 130 × 130 grid. Figure 10 provides similar comparison for the four-sided lid-driven cavity. Expectedly a 4-level multigrid cycle shows a faster convergence than a single grid. As for single lid-driven cavity, the residuals in the two- and four-sided cavities falls faster at the beginning and this slows down thereafter whereas in the multigrid method the residual falls at a more or less the constant rate.



(a) Re = 1500

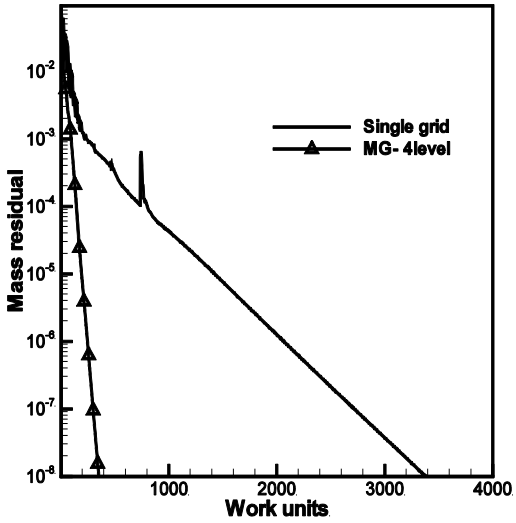


(b) Re = 2000

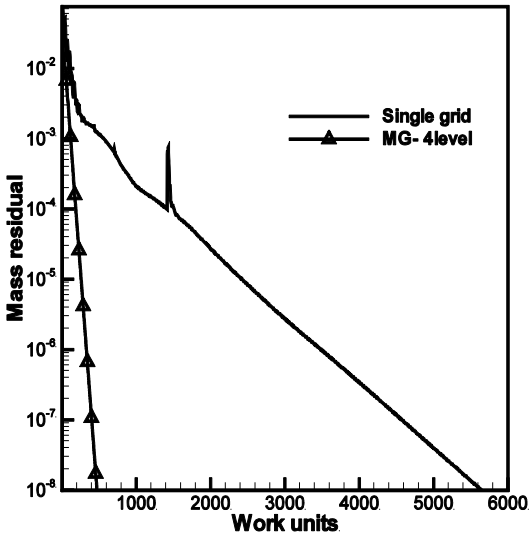
Fig. 9 Mass residual history of multigrid methods for a two-sided lid-driven cavity.

Tables 2 and 3 summarize the total CPU time required and speed-up obtained by the multigrid for 2-sided and 4-sided cavity flows, respectively. It can be seen that the time-wise speed-up achieved by the multigrid is approximately 9 to 10 times. Thus in terms of computational efficiency, the multigrid method is substantially faster than the single-grid method. It may be noted that multigrid pay-off is likely to be higher

for finer grids. These tables exemplify the excellent potential of the multigrid technique for accelerating the convergence even for flow geometries giving multiple solutions.



(a) Re = 100



(b) Re = 200

Fig. 10 Mass residual history of multigrid methods for a four-sided lid-driven cavity.

Table 2 Performance of multigrid method for a two-sided lid-driven cavity flow at various Reynolds numbers.

Reynolds number	CPU time (minutes) Single-grid	MG 4-level	Speed-up
1500	325	32	10.15
2000	451	42	10.73

Table 3 Performance of multigrid method for a four-sided lid-driven cavity flow at various Reynolds numbers.

Reynolds number	CPU time (minutes) Single-grid	MG 4-level	Speed-up
100	172	18	9.55
200	202	22	9.18

4.0 CONCLUSIONS

A full-approximation storage (FAS) multigrid code using the finite volume method and SIMPLE algorithm on a colocated grid arrangement is developed to obtain stable multiple solutions for two- and four-sided lid-driven cavities. Since the convective terms in the Navier-Stokes equations are discretized using the QUICK scheme and the viscous terms are central-differenced to second-order accuracy, the code offers accurate spaatial resolution. To establish the credibility and performance of the code, it is first used to compute the flow in a standard 2D single-lid-driven cavity to demonstrate that the results closely match with the corresponding highly reliable existing results. Ability of the 4-level multigrid method to obtain speed-up of 8 to 10 compared with the single-grid method exhibits the good time-wise performance of the code. After having thus gained an insight into various aspects of the code it is then used to compute the flows in two- and four-sided 2D lid-driven cavities. These two flow configurations exhibit many interesting flow features which include multiple stable solutions. It is established that the solutions valid and stable. It may be noted that nonlinear problems are known at times to give multiple solutions and the traditional mathematical concept of wellposedness does not apply here. For the first time a multigrid technique is used to compute the solutions for such peculiar fluid-mechanical situations with substantial time-wise acceleration of convergence.

REFERENCES

Albensoeder S., Kuhlmann H. and Rath H. 2001. Multiplicity of steady two-dimensional flows in two-sided lid-driven cavities, Theoretical and Computational Fluid Dynamics, **14:** 223–41.

Alleborn N., Raszillier H. and Durst F. 1999. Lid-driven cavity with heat and mass transport, International Journal of Heat and Mass Transfer, **42:** 833–53.

Auteri F., Parolini N. and Quartapelle L. 2002. Numerical investigation on the stability of singular driven cavity flow. Journal of Computational Physics, **183:** 1–25.

Barragy E. and Carey G. 1997. Streamfunction vorticity driven cavity solution using p finite elements. Computers and Fluids, **26:** 453–68.

Botella B. and Peyret R. 1998. Benchmark spectral results on the lid-driven cavity flow. Computers and Fluids **27:** 421–33.

Brandt A. 1977. Multilevel adaptive solutions to boundary-value problems, Mathematics of Computation, **31:** 333–90.

Bruneau C. and Jouron C. 1990. An efficient scheme for solving steady incompressible NavierStokes equations. Journal of Computational Physics, **89:** 389–13.

Bruneau C. and Saad M. 2006. The 2D lid-driven cavity problem revisited. Computers and Fluids, **35:** 326–48.

Cadou J.M., Guevel Y. and Girault G. 2012. Numerical tools for the stability analysis of 2D flows: application to the two- and four-sided lid-driven cavity, Fluid Dynamics Research, **44:** doi:10.1088/0169-5983/44/3/031403

Erturk E., Corke T. and Gokcol C. 2005. Numerical solutions of 2-D steady incompressible driven cavity flow at high Reynolds numbers.International Journal for Numerical Methods in Fluids, **48:** 747–74.

Fedorenko R. 1962. A relaxation method for solving elliptic difference equations, Computational Mathematics and Mathematical Physics, **1:** 1092–96.

Fedorenko R. 1964. The speed of convergence of one iteration process Computational Mathematics and Mathematical Physics, **4**, 227–35.

Ghia U., Ghia K. and Shin C. 1982. High-Resolutions for incompressible Navier-Stokes equation and a multigrid method. Journal of Computational Physics, **48:** 387–411.

Hackbusch W. 1978. On the multigrid method applied to difference equation, Computing, **20:** 291–306.

Hayase T., Humphrey J.A.C. and Grief R. 1992. A consistently formulated QUICK scheme for fast and stable convergence using finite-volume iterative calculation procedures. Journal of Computational Physics, **98:** 108–18.

Hortmann M. and Peric M. 1990, Finite volume multigrid prediction of laminar natural convection:Bench-mark solutions. International Journal for Numerical Methods in Fluids, **11:** 189–207.

Kalita J., Dalal D. and Dass A. 2002. A class of higher order compact schemes for the unsteady two-dimensional convection diffusion equation with variable convection coefficients.International Journal for Numerical Methods in Fluids, **38:** 1111–31.

Kuhlmann H., Wanschura M. and Rath H. 1997. Flow in two-sided lid-driven cavities: Nonuniqueness, instabilities, and cellular structures, Journal of Fluid Mechanics, **336:** 267–99.

Kuhlmann H., Wanschura M. and Rath H. 1998. Elliptic instability in two-sided lid-driven cavity flow, European Journal of Mechanics - B/Fluids, **17:** 561–69.

Leonard B. 1979. A stable and accurate convective modeling procedure based on quadratic upstream interpolation, Computing Methods in Applied Mechanics and Engineering, **19:** 59–98.

Lien F. and Leschziner M. 1994. Multigrid acceleration for recirculating laminar and turbulent flows computed with a non-orthogonal collocated finite volume scheme.Computational Methods in Applied Mechanics and Engfineering, **118:** 351-71.

Luo W. and Yang R. 2007. Multiple fluid flow and heat transfer solutions in a two-sided liddriven cavity, International Journal of Heat and Mass Transfer, **50:** 2394–405.

Namprai A. and Witayangkurn S. 2012. Fluid Flow and heat transfer in square cavities with discrete two source-sink pairs, Advanced Studies in Theoritical Physiscs, **6:** 743-53.

Patankar S. and Spalding D. 1972. A calculation procedure for heat, mass and momentum transfer in three-dimensional parabolic flows, International Journal of Heat and Mass Transfer, **15:** 1787–806.

Rhie C. and Chow W. 1983. A numerical study of the turbulent flow past an iosolated airfoil with trailing edge separation. AIAA Journal, **21:** 1525–32.

Santhosh K.D., Dass A.K. and Dewan A. 2009. Analysis of Non-Darcy Models for Mixed Convection in a Porous Cavity Using a Multigrid Approach, Numerical Heat Transfer, Part A, **56:** 685-708.

Sivaloganathan S. and Shaw G. 1988. A multigrid method for recirculating flows, International Journal for Numerical Methods in Fluids, **8:** 417–40.

Wahba E. 2009. Multiplicity of states for two-sided and four-sided lid driven cavity flows. Computers and Fluids, **38:** 247–53.

Yan J. and Thiele F. 1998. Performance and accuracy of a modified full multigrid algorithm for fluid flow and heat transfer.Numerical Heat Transfer: Part B, **34:** 323–38.